

# Preparation and characterization of nanostructured nickel oxide thin films by spray pyrolysis

Raid A. Ismail · Sa'ad Ghafari · Ghada A. Kadhim

Received: 16 June 2012 / Accepted: 27 July 2012 / Published online: 18 August 2012  
© The Author(s) 2012. This article is published with open access at Springerlink.com

**Abstract** Transparent crystalline nanostructured nickel oxide (NiO) thin films were prepared using a simple spray pyrolysis technique from hydrated nickel chloride salt solution ( $\text{NiCl}_2 \cdot 6\text{H}_2\text{O}$ ) onto glass and silicon (n-type) substrates at different temperatures (280, 320, 360, and 400 °C) and with different solution concentrations (0.025, 0.05, 0.075, and 0.1 M). Structural and morphological properties of the grown NiO films were studied using X-ray diffraction (XRD) and atomic force microscope. Optical properties and chemical analysis of the films were characterized by UV–visible absorption spectra and Fourier transform infrared spectroscopy, respectively. The XRD result showed that the deposited film has an amorphous structure when deposited at temperature of  $T_s = 280$  °C and concentration of 0.025 M. At higher temperatures ( $T_s = 320, 360, 400$  °C) and solution concentrations (0.05, 0.075, 0.1 M), the deposited films have cubic polycrystalline structure formed with preferred orientation along (111) plane. The band gap of NiO film increases from 3.4 to 3.8 eV as the molarity decreased from 0.1 to 0.05 M.

**Keywords** Nanostructure · Nickel oxide · Spray pyrolysis · Optical properties XRD · AFM

## Introduction

Transparent conducting oxides (TCO) thin films such as Sn-doped  $\text{In}_2\text{O}_3$ , Al-doped ZnO and Sb-doped  $\text{SnO}_2$  are attracting more and more attention due to their wide applications such as liquid crystal displays, light-emitting diodes, solar cells and detectors (Wager 2003; Hosono et al. 2002). These traditional TCOs often show n-type conductivity but there is lack of p-type TCO. Nickel oxide (NiO) is a p-type TCO with an energy gap of 3.4–3.8 eV (Sato et al. 1993), with gray coloration. NiO thin films adopt the NaCl structure, with octahedral (Ni) (II) and ( $\text{O}^{2-}$ ) sites. They are recently drawing considerable attention because of their importance in several scientific and technological applications. They have lots of special optical, electrical and magnetic properties. They are used as anti-ferromagnetic materials (Rong et al. 2010), and for electrochromic display devices (Youshmura et al. 1995). In addition, they are employed as a part of functional sensor layers in chemical sensors (Kumagai et al. 1996), and used in batteries (Puspharajah et al. 1997), fuel cell (Wang et al. 2002), electrochromic devices (Agrawal et al. 1992), solar thermal absorber (Tanaka et al. 1996), catalyst for oxygen evolution (Yeh and Matsumura 1997) and photo electrolysis (Bonger et al. 1998). Several physical and chemical methods, such as sputtering (Nandy et al. 2010), pulsed laser deposition (Xia et al. 2008), chemical bath deposition (Wang et al. 2012) and sol–gel (Al-Ghamdi et al. 2009) have been adopted to prepare NiO films. Spray pyrolysis is simple, low cost and feasible for mass production. This paper presents the preparation of nanostructured NiO thin films by spray pyrolysis technique (SPT) using hydrated nickel chloride salt solutions ( $\text{NiCl}_2 \cdot 6\text{H}_2\text{O}$ ) onto glass and silicon (n-type) substrates. The second objective of this work is to study the effect of molarity and substrate

R. A. Ismail (✉)  
Applied Science Department, University of Technology,  
Baghdad, Iraq  
e-mail: raidismail@yahoo.com

S. Ghafari · G. A. Kadhim  
College of Science for Women, University of Baghdad,  
Baghdad, Iraq

temperature on the optical, structural, morphological and electrical characteristics of NiO films.

### Experimental details

Nickel oxide thin films were deposited from aqueous solution of AR grade nickel chloride ( $\text{NiCl}_2 \cdot 6\text{H}_2\text{O}$ ), by SPT on corning glass and single crystal silicon substrates. The substrates have been chemically and ultrasonically cleaned by standard methods. Nickel chloride solution was sprayed onto the preheated glass and silicon substrates, which undergoes evaporation, solute precipitation and pyrolytic decomposition, thereby resulting in nickel oxide thin films according to the following reaction:



The prepared films were gray, uniform and strongly adherent to the substrates. The thickness of the films was varied from 0.215 to 0.91  $\mu\text{m}$ . In order to get uniform thin films, the height of the spraying nozzle and the rate of spray process were kept constant during the deposition process at 35 cm and 15  $\text{cm}^3/\text{min}$ , respectively. The spraying process lasted about 6 s. The period between spraying processes was about 1 min; this period was enough to avoid excessive cooling of the substrate. Thermocouple was fixed to the substrate's surface and the temperature was measured at the four corners of the glass substrate surface, then the results were averaged and the standard deviation was calculated ( $\pm 5^\circ\text{C}$ ). The films were prepared by spraying a (0.025, 0.05, 0.075 and 0.1 M) solution of nickel chloride in 30 ml distilled water onto substrates at different temperatures (280, 320, 360 and 400  $^\circ\text{C}$ ). NiO film was deposited on silicon substrate at a temperature of 400  $^\circ\text{C}$  and a concentration of 0.075 M. The structural properties of the film were investigated using X-ray diffractometer (XRD, Shimadzu-6000) using  $\text{Cu K}_\alpha$  radiation. The morphology of the film was studied using atomic force microscope (AFM) (Angstrom AA3000), while the atomic bonds in NiO were analyzed with the Fourier transformed infrared spectroscope (FT-IR, Shimadzu IR Affinity-1). The optical transmittance of the films was measured using UV–vis spectrophotometer (Union space international Uv1601) in the spectral range 300–900 nm. The film thickness was measured by the gravimetric method and Hall measurements were carried out to investigate the mobility and conductivity type of the deposited film.

### Results and discussion

Figures 1 and 2 display the XRD spectra of the films deposited at different molarities and temperatures. All the

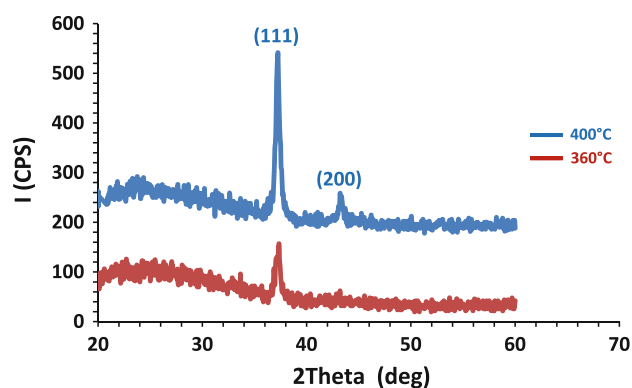


**Fig. 1** XRD patterns for the NiO films prepared at different substrate temperatures and 0.05 M

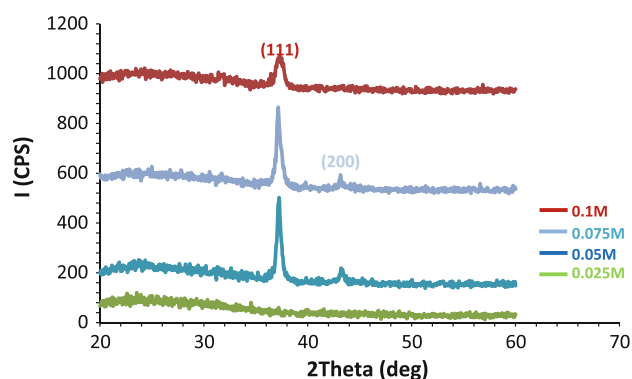


**Fig. 2** XRD patterns for the NiO films prepared at different solution concentrations

grown films at 400  $^\circ\text{C}$  are crystalline in nature and all the diffracted peaks observed in XRD spectra belong to the cubic NiO phase, while the film prepared at 0.025 M was amorphous. The XRD pattern of the NiO film grown at 360  $^\circ\text{C}$  has a single diffracted peak along (111) plane corresponding to  $2\theta = 37^\circ$ . The intensity of the (111) plane increases as the substrate temperature increases from 360 to 400  $^\circ\text{C}$ . Besides, there is a weak reflection plane noticed along the (200) plane at  $2\theta = 43^\circ$ . The substrate temperature controls the mobility of the deposited atoms. As substrate temperature increases, the adsorbed atoms gain extrathermal energy and move to another preferred plane. The value of lattice constant for (111) plane was found to be 0.417 nm which is very close to that for bulk NiO taken from JCPDS file # 04-0835. The good agreement between observed and standard lattice constant values confirms the growth of NiO. No other phases were noticed in the XRD spectra. The XRD spectrum showed that the NiO film synthesized with a concentration of 0.025 M was amorphous. Decreasing the substrate temperature to 350  $^\circ\text{C}$  results in a decrease in the intensity of the (111) plane, as well as the disappearance of (200) plane. XRD

results confirm the crystallinity improvement of the film with the increase of molar concentration up to 0.075 M. This result indicates that the texturation of the film is higher when the precursor molar concentration is larger. XRD spectrum of NiO film prepared with 0.1 M showed single diffracted peak along (111) plane, the full width at half maximum is increased and disappearance of (200) plane is due to increasing concentration of lattice imperfection coming from the internal microstrain within film. The grain size (GS) of crystallite was calculated for (111) plane using Scherrer's formula:

$$GS = \frac{0.9\lambda}{\beta \cos \theta} \quad (2)$$

where  $\lambda$  is wavelength (0.154 nm) and  $\beta$  is the FWHM of the X-ray peak. Table 1 reveals that the GS of the film decreases with the increase of molar concentration. A typical XRD pattern, shown in Fig. 3, reveals the crystalline nature of the NiO film deposited on monocrystalline silicon substrate at 400 °C. It is clear from this figure that the film is crystalline and the preferred orientation changed from (111) to (200).

Films deposited onto silicon (n-type) at 400 °C and 0.075 M, were examined and found to have higher degree of crystallization than when deposited on glass, as shown in Fig. 3.

It is clear from Fig. 3 that the NiO film deposited on Si has preferred orientation along (200) plane, and this can be ascribed to formation and epitaxial growth of NiO on Si.

**Table 1** Surface roughness as function of concentration determined from AFM

Molar concentration (M)	Average roughness (nm)	RMS roughness (nm)
0.05	3.5	4.5
0.075	2	2.5
0.1	1.1	1.4

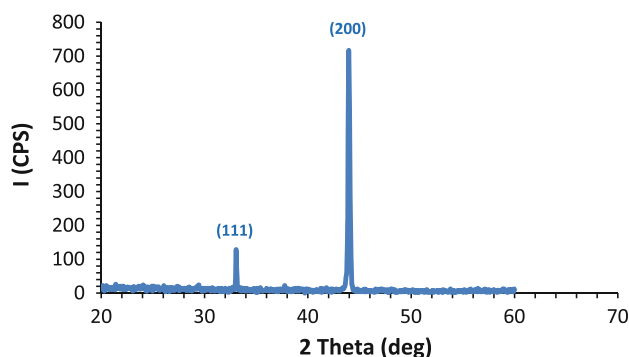


**Fig. 3** XRD spectrum for the NiO films deposited on silicon and prepared at 400 °C and 0.075 M

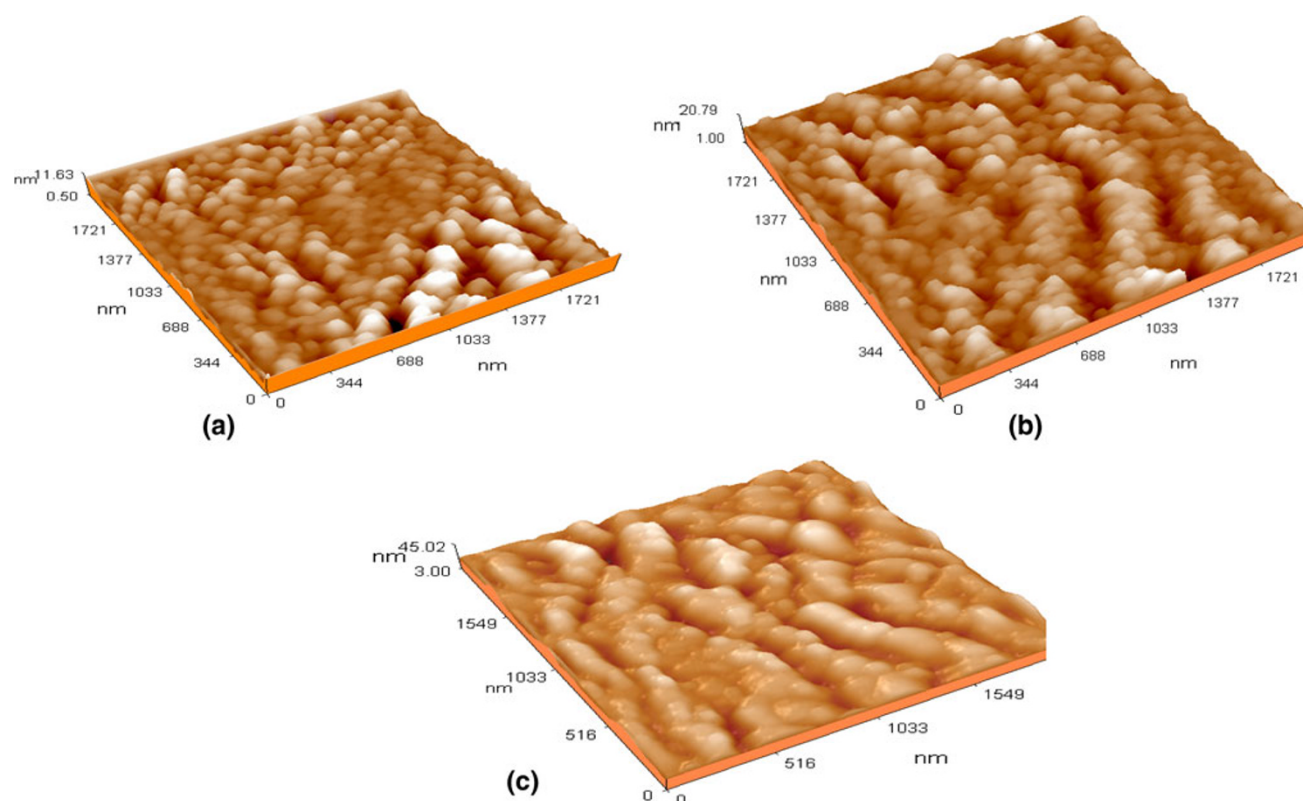
The morphological investigation of NiO films deposited on glass at 400 °C with various molar concentrations was accomplished by using AFM. Typical 3D AFM images of the NiO films synthesized at different molar concentrations are shown in Fig. 4. AFM results showed homogenous and smooth NiO films. The average crystallite size, average roughness and root mean square (RMS) roughness for NiO, estimated from AFM, are given in Table 1. Higher molar concentration has decreased the crystallite size and RMS roughness of the film. The increase of the crystallite size may be caused by columnar grain growth in the structure. The results of crystallite size obtained from AFM investigation are in good agreement with those obtained from XRD measurements shown in Table 2.

Figure 5 shows the granularity distribution chart of the NiO film prepared with 0.05 M, it is clear that the film has different GS (from 70 to 160 nm) and the average GS is approximately 115.1 nm.

FT-IR transmission spectrum of the NiO thin film prepared at 400 °C with 0.075 M in the range between 400 and 2,000  $\text{cm}^{-1}$  is shown in Fig. 6. The bands at 611.43, 875.65, 1,422, 1,745, 3,776  $\text{cm}^{-1}$  are assigned to Ni–O interaction (Romero et al. 2010). The other bands clearly indicate that the sample consists of water molecules and/or hydroxide ions and their presence in the IR spectrum may be due to the absorption of water. The FT-IR spectra for the NiO films prepared at other molar concentrations showed the same absorption peaks but with lower intensities.

The band at 1,300  $\text{cm}^{-1}$  is attributed to the bending vibration of water molecule due to the absorbed moisture. The transmittance of nanostructured NiO films, deposited on glass substrates, prepared at various molarities is presented in Fig. 7. All films synthesized at different molarities displayed high transparency in visible and near IR regions with little difference in optical transparency. The optical confinement effect was noticed around 325 nm for NiO film prepared at 0.075 M. Figure 8 shows the plot of  $(\alpha h\nu)^2$  versus  $h\nu$  for NiO films deposited at different molarities. The optical band gap can be obtained from extrapolating the straight line of the plot to  $\alpha = 0$  (direct transition). The value of optical band gap shifts towards the lower energy and the slope of the plot decreases when the molar concentration increases. The optical band gap changed from 3.4 to 3.8 eV when the concentration decreased from 0.1 to 0.05 M. This result can be ascribed to the increasing crystallite size with the decrease of molar concentration of the film (Makhlouf et al. 2010). The large value of band gap of the NiO film is due to quantum size effect (Romero et al. 2010).

Hall measurements revealed p-type NiO films and at the room temperature electrical resistivity of these films increased from  $4.39 \times 10^3$  to  $8 \times 10^3 \Omega \text{ cm}$ , as the molar concentration increased from 0.05 to 0.1 M. This is due to



**Fig. 4** 3D AFM images of nanostructured NiO thin films **a** 0.1 M, **b** 0.075 M and **c** 0.05 M

**Table 2** Values of the grain size (GS) calculated from XRD and AFM investigations

Molar concentration (M)	GS (XRD measurement) (nm)	Average GS (AFM investigation) (nm)
0.05	110.7	115.1
0.075	76	84
0.1	78	80

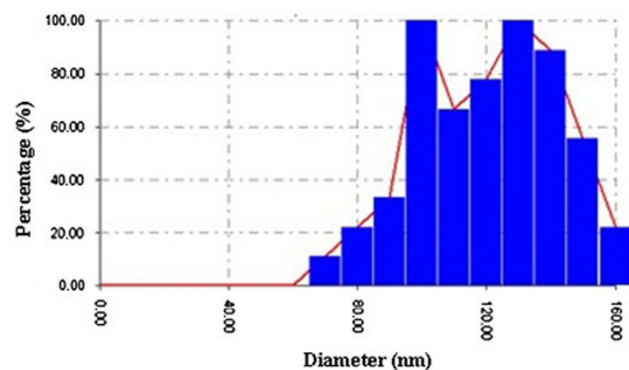


**Fig. 5** Granularity distribution of nanostructured NiO film prepared at 0.05 M

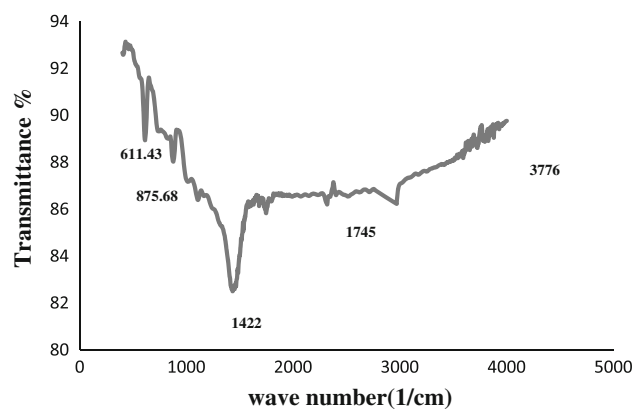


**Fig. 6** FT-IR spectrum of the NiO thin film synthesized at 400 °C and 0.075 M

the thickness increase, non-stoichiometry and surface state (Romero et al. 2010). The values of electrical resistivity found here are lower than that for pure and stoichiometric NiO. It is reported that the formation of non-stoichiometry with excess or less oxygen results in the reduction of resistivity through the doping process (Patil and Kadam 2002). The variation of electrical resistivity with temperature for the NiO films deposited at different molarities is

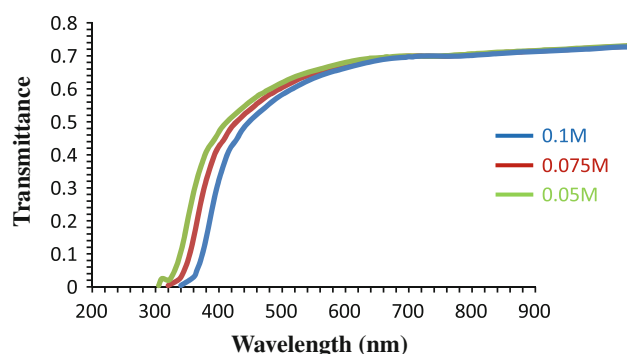


**Fig. 7** Transmittance spectra of the NiO films prepared at 400 °C with different concentrations

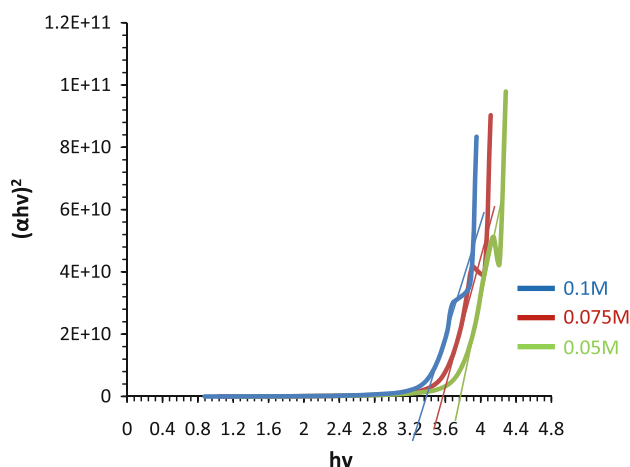


**Fig. 8**  $(\alpha h\nu)^2$  versus  $(h\nu)$  plot

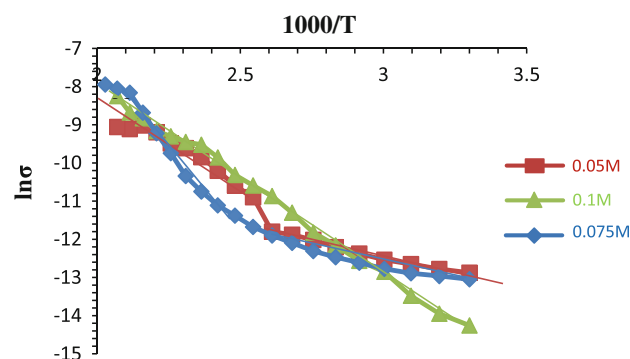


**Fig. 9** Electrical resistivity as function of temperature

**Table 3** Lists the dependence of activation energy on film concentration

Molar concentration (M)	Activation energy ( $E_1$ ) (eV)	Activation energy ( $E_2$ ) (eV)
0.05	0.14	0.14
0.075	0.13	0.13
0.1	0.08	0.25

demonstrated in Fig. 9. It is obvious from this figure that the resistivity decreases with the temperature increase, which confirms the semiconducting nature of NiO film. Arrhenius equation was used to estimate the activation energy of deposited films. Table 3 lists the thermal activation energy as a function of molar concentration. The dislocation and stoichiometry arising from the difference in experimental conditions play major role in varying the activation energy with concentration. The film mobility was found to be approximately  $5.5 \times 10^2 \text{ cm}^2 \text{ V}^{-1} \text{ s}^{-1}$ .

## Conclusion

Cubic nanostructured NiO films were deposited by spray pyrolysis of  $\text{NiCl}_2 \cdot 6\text{H}_2\text{O}$ . The properties of the films depend on molar concentration and substrate temperature. The film thickness increased from 0.21 to 0.91  $\mu\text{m}$  as molar concentration was varied from 0.025 to 0.1 M. The AFM investigation showed a decreasing RMS film roughness when increasing the molar concentration. XRD studies revealed that the NiO films deposited on glass substrate with molar concentration higher than 0.025 M are polycrystalline with preferred orientation along (111) plane, while films deposited on silicon substrate were polycrystalline too but with preferred orientation along (200) plane. The optical band gap of the NiO films changed from 3.4 to 3.8 eV as molar concentration decreased from 0.1 to 0.05 M, which indicated that it is dependent on the film stoichiometry. The electrical resistivity of the deposited NiO films increased as concentration increased.

**Open Access** This article is distributed under the terms of the Creative Commons Attribution License which permits any use, distribution, and reproduction in any medium, provided the original author(s) and the source are credited.

## References

- Agrawal A, Habibi HR, Agrawal RK, Cronin JP, Roberts DM, R'Sue CP, Lampert CM (1992) Effect of deposition pressure on the microstructure and electrochromic properties of electron-beam-evaporated nickel oxide films. *Thin Solid Films* 22:239–253
- Al-Ghamdi A, Mahmoud W, Yaghmour S, Al-Marzouki F (2009) Structure and optical properties of nanocrystalline NiO thin film synthesized by sol-gel spin coating method. *J Alloy Compd* 486:9–13
- Bonger M, Fuchs A, Schamagl K, Winter R, Doll T, Eisele I (1998) Thin  $(\text{NiO})_{1-x}(\text{Al}_2\text{O}_3)_x$ , Al-doped and Al coated NiO layers for gas detection with HSGFET. *Sens Actuators B* 47:145–152
- Hosono H, Ohta H, Orita M, Ueda K, Hirano M (2002) Frontier of transparent conductive oxide thin films. *Vacuum* 66:419–425
- Kumagai H, Matsumoto M, Toyoda K, Obara M (1996) Preparation and characteristics of nickel oxide thin film by controlled growth with sequential surface chemical reactions. *J Mater Sci Lett* 15:1081–1083



- Makhlouf S, Kassem M, Abedulrahim M (2010) Crystallite size dependent optical properties of nanostructured NiO films. *J Optoelectron Adv Mater* 4:1562
- Nandy S, Goswami KS, Chattopadhyay K (2010) Ultra smooth NiO thin film on flexible (PET) substrate at room temperature by RF magnetron sputtering and effect of oxygen partial pressure on their properties. *Appl Surf Sci* 256:3142–3147
- Patil P, Kadam L (2002) Preparation and characterization of spray pyrolyzed nickel oxide (NiO) thin films. *Appl Surf Sci* 199:211–221
- Puspharajah P, Radhakrishna S, Arof AK (1997) Transparent conducting lithium-doped nickel oxide thin films by spray pyrolysis technique. *J Mater Sci* 32:3001–3006
- Romero R, Martin F, Ramos-Barrado JR, Leinen D (2010) Synthesis and characterization of nanostructured nickel oxide thin films prepared. *Thin Solid Films* 518:4499–4502
- Rong X, Xin W, Delong J, Junqiao L, Guozheng W, Ye L, Qingduo D, Jingquan T (2010) Structural and photoelectrical properties of NiO thin film. *Chin J Electron* 19:631–633
- Sato H, Minami T, Takata S, Yamada T (1993) Transparent conductive p-type NiO thin-films prepared by magnetron sputtering. *Thin Solid Films* 236:27–31
- Tanaka M, Mukai M, Fujimori Y, Kondoh M, Tasaka Y, Baba H, Usami S (1996) Transition metal oxide films prepared by pulsed laser deposition for atomic beam detection. *Thin Solid Films* 281:453–456
- Wager J (2003) Transparent electronics. *Science* 300:1245–1246
- Wang SY, Wang W, Wang WZ, Du YW (2002) Preparation and characterization of highly oriented NiO (200) films by a pulse ultrasonic spray pyrolysis method. *Mater Sci Eng B* 90:133–137
- Wang H, Wang Y, Wang X (2012) Pulsed laser deposition of NiO thin film at room temperature for high-rate pseudocapacitive energy storage. *Electrochem Commun* 18:92–95
- Xia X, Tu J, Zahang J, Wang X, Zahang W, Huang H (2008) Electrochromic properties of porous NiO thin films prepared by CVD. *Sol Energy Mater Sol Cells* 92:628–633
- Yeh WC, Matsumura M (1997) Chemical vapor deposition of nickel oxide films from bis-pi-Cyclopentadienyl-nickel. *Jpn J Appl Phys* 36:6884–6887
- Yoshimura K, Miki T, Tanemura S (1995) Nickel oxide electrochromic thin films prepared by reactive dc magnetron sputtering. *Jpn J Appl Phys* 34:2440–2446

